Quantum electrodynamics near an interface

J. M. Wylie and J. E. Sipe
Department of Physics and Erindale College, University of Toronto, Toronto, Ontario, Canada M5S 1A7
(Received 28 February 1984)

A quantum-mechanical linear-response formalism is used to calculate the frequency shift and lifetime of an excited atom near an arbitrary flat interface. The results depend on the frequency-dependent atom and field susceptibilities, and in the vicinity of an interface can be expressed in terms of the appropriate Fresnel reflection coefficients; the contributions from surface excitations are easily identified. As examples, we consider an atom above a metal and a dielectric waveguide.

I. INTRODUCTION

Recent work on the behavior of atoms and molecules at surfaces has led to a renewed interest in quantum electrodynamics in the presence of an interface.[1-3] Two standard problems, the lifetime and frequency shift of an atom in an excited state near a perfectly conducting surface, have a long history which we will not review here. The usual solution[1,4] involves quantizing the radiation field through mode expansions appropriate to a half-space of vacuum bounded by a perfect conductor. Although showing in detail the effect of the conductor on the radiation field, this approach is algebraically complicated and does not clearly exhibit the similarity of this problem with, for example, that of an atom in the presence of another atom, rather than a surface. Further, the generalization to a dielectric or even a waveguide surface is not straightforward.

An alternate approach, presented by McLachlan,[5,6] involves casting expressions for the lifetimes and frequency shifts in forms involving correlation functions that appear in linear-response theory. These results have a transparent physical interpretation and in principle can be used with any model for the neighboring surface (or neighboring atom). A related approach by Agarwal[7,8] was applied to an atom in the vicinity of a surface, but his results were shown to have quantum-mechanical inconsistencies.[4] As well, Agarwal's results are not of a form that can be easily generalized to, say, an atom in the presence of a multilayer geometry.

The difficulty in using a linear-response formalism lies in calculating the field susceptibility functions for surface geometries. Mehl and Schaich[2] described the effects of the surface by introducing complex impedances. In this paper we show that the surface effects of interest depend only on the appropriate Fresnel coefficients and that, in particular, the contribution of any surface excitations can easily be investigated since they are signaled by poles in those coefficients. By constructing expressions for level shifts and lifetimes in terms of Fresnel coefficients, we obtain a more general formalism than those of earlier authors; we can treat multilayer geometries using, if required and desired, results from microscopic theory for the response of the surface to electromagnetic fields. We demonstrate our methods by calculating the lifetimes and frequency shifts of atoms near a metallic surface and near a dielectric waveguide. We also recover the now well-known expressions for the lifetimes and frequency shifts of an atom above a perfect conductor,[1,4] in a manner that is simpler than most other derivations and that displays the relation of this ideal model to more realistic problems.

The organization of the paper is as follows. In Sec. II we briefly show how lifetimes and frequency shifts may be written in terms of frequency-dependent atom and field susceptibilities. As have most earlier workers,[1-8] we restrict ourselves to cases where charge overlap between the atom and the surface can be neglected. Since this part of the formalism has been developed earlier, we refer freely to results in the literature and only outline the derivation, casting the final expressions in a form that is suitable for our further use. We work with the multipolar form of the interaction Hamiltonian[1,9] and keep only terms due to dipole transitions, although this restriction could be easily removed. In Sec. III we outline the Fresnel coefficient method of calculating the field susceptibilities for surface geometries. Our final results for lifetimes and level shifts, which are applicable to an arbitrary interface, constitute a significant generalization and simplification of earlier expressions. In Sec. IV we recover the well-known expressions[1,4,8] for a single atom above a perfectly conducting surface. In Secs. V and VI we calculate the lifetimes and level shifts for a single atom above a metal and a dielectric waveguide, respectively. Specifically, we consider a sodium surface, a glass surface, and a ZnO/sapphire waveguide. Our conclusions and the nature of our contribution are reviewed in Sec. VII.

II. TRANSITION RATES AND FREQUENCY SHIFTS IN THE DIPOLE APPROXIMATION

We consider an atom interacting with the radiation field through the interaction Hamiltonian[1,9,10]

$$H_I = -\vec{\mu}\cdot\vec{D}(\vec{r}_0) \tag{2.1}$$

where $\vec{\mu}$ is the dipole operator of an atom at position $\vec{r}_0$, and $\vec{D}(\vec{r})$ is the transverse displacement field. In writing Eq. (2.1) we neglect multipole moments of the charge distribution higher than the electric dipole; we have also omitted a term involving the transverse part of the microscopic polarization field,[1] which only leads, in the low or-

ders of perturbation theory we consider, to a contribution to the nonrelativistic free space Lamb shift.[9,11] In first order, the transition rate from an initial atomic state $|i\rangle$ to a final state $|f\rangle$ is given by Fermi's golden rule,

$$R_{fi}=\frac{2\pi}{\hbar}\sum_{I,F}p(I)\,|\langle F|\langle f|\vec{\mu}\cdot\vec{D}(\vec{r}_0)|i\rangle|I\rangle|^2 \times\delta(E_F+E_f-E_I-E_i)\,, \tag{2.2}$$

where capital letters denote eigenstates of the rest of the total system under consideration, neglecting its interaction with the atom of interest. Such eigenstates might involve, and depend on the coupling between, the radiation field, other atoms, surface excitations, and the like. For convenience, we refer to these as "field states." For simplicity we assume here that the field is in thermal equilibrium at a temperature T; $p(I)=\exp(-\beta E_I)/\sum_K\exp(-\beta E_K)$, with $\beta=(k_BT)^{-1}$, is then the probability that the field is in state I.

Expressing the δ function in (2.2) in integral form, we find

$$R_{fi}=\frac{1}{\hbar^2}\int_{-\infty}^{+\infty}dt\,\langle D_\alpha(\vec{r}_0,t)D_\beta(\vec{r}_0,0)\rangle\mu_\alpha^{fi}\mu_\beta^{if}\exp(i\omega_0 t)\,, \tag{2.3}$$

where $\omega_0=(E_f-E_i)/\hbar$, the Greek subscripts denote Cartesian components and are to be summed over when repeated, and $\mu_\alpha^{fi}=\langle f|\mu_\alpha|i\rangle$, etc. In Eqs. (2.3) and (2.4), $D_\alpha(\vec{r}_0,t)$ is an interaction picture operator, evolving as if (2.1) were not present, and the angular brackets indicate an ensemble average. Defining a correlation function

$$G_{\alpha\beta}(\vec{r},\vec{r}';t)=\frac{i}{\hbar}\langle[D_\alpha(\vec{r},t),D_\beta(\vec{r}',0)]\rangle\Theta(t)\,, \tag{2.4}$$

where $\Theta(t)$ is the usual unit-step function, we may use the fluctuation-dissipation theorem[7,12] to rewrite Eq. (2.3) as

$$R_{fi}=\frac{2\mu_\alpha^{fi}\mu_\beta^{if}\mathrm{Im}G_{\alpha\beta}(\vec{r}_0,\vec{r}_0;\omega_0)}{\hbar[1-\exp(-\beta\hbar\omega_0)]}\,, \tag{2.5}$$

where

$$G_{\alpha\beta}(\vec{r},\vec{r}';\omega)=\int_{-\infty}^{+\infty}dt\,G_{\alpha\beta}(\vec{r},\vec{r}';t)\exp(i\omega t)\,. \tag{2.6}$$

The temperature dependence, which appears in the form of an occupation number, will be important only for $k_BT\geq\hbar\omega_0$. Since we are here interested primarily in atomic transition energies on the order of a Rydberg, we can set $T=0$ K in Eq. (2.5).

Turning now to energy-level shifts, we start with the usual second-order perturbation expression for the energy shift of the ath atomic level due to the interaction (2.1),

$$\delta E_a=-\frac{P}{\hbar}\sum_{B,N,m}p(B)\frac{D_\alpha^{BN}(\vec{r}_0)D_\beta^{NB}(\vec{r}_0)\mu_\alpha^{am}\mu_\beta^{ma}}{(\omega_N-\omega_B)+(\omega_m-\omega_a)}\,, \tag{2.7}$$

where P denotes the principal part. The reduction of Eq. (2.7) is greatly simplified by introducing positive- and negative-frequency parts of the field $\vec{D}(\vec{r},t)$,[7]

$$D_\alpha^{\pm}(\vec{r},t)=\frac{1}{2\pi}\int_0^\infty d\omega\,D_\alpha(\vec{r},\pm\omega)\exp(\mp i\omega t) \tag{2.8}$$

and where, as before, the time evolution is in the interaction picture. Going back to the Schrödinger picture in Eq. (2.7), it is easy to see that terms of the form $(D_\alpha^{\pm})^{BN}(D_\beta^{\pm})^{NB}$ will not contribute (cf. Ref. 7), and we may introduce a δ function to write

$$\delta E_a=-\frac{P}{\hbar}\sum_{B,N,m}p(B)\int_{-\infty}^{+\infty}d\omega\frac{[D_\alpha^{+BN}(\vec{r}_0)D_\beta^{-NB}(\vec{r}_0)+D_\alpha^{-BN}(\vec{r}_0)D_\beta^{+NB}(\vec{r}_0)]}{\omega+(\omega_m-\omega_a)}\mu_\alpha^{am}\mu_\beta^{ma}\delta(\omega-\omega_N+\omega_B)\,. \tag{2.9}$$

Restricting ourselves to $T=0$ K as above, a further simplification is possible using the identity[7]

$$\sum_{N,B}p(B)D_\alpha^{\mp BN}(\vec{r})D_\beta^{\pm NB}(\vec{r}')\delta(\omega-\omega_N+\omega_B) =\frac{\hbar}{\pi}\mathrm{Im}G_{\alpha\beta}(\vec{r},\vec{r}';\omega)\Theta(\mp\omega)\,, \tag{2.10}$$

which follows immediately from the definitions of $G_{\alpha\beta}$ and $D_\alpha^{\pm}$. Introducing a molecular correlation function,

$$\alpha_{\alpha\beta}^a(t)=\frac{i}{\hbar}\langle a|[\mu_\alpha(t),\mu_\beta(0)]|a\rangle\Theta(t) \tag{2.11}$$

and writing down the identity analogous to (2.10) for $\alpha_{\alpha\beta}^0(\omega)$, we find that for the *atom* also at $T=0$ K (ground state) Eq. (2.9) can be written as

$$\delta E_0=-\frac{\hbar P}{\pi^2}\int_0^\infty\int_0^\infty d\omega\,d\omega'\frac{\mathrm{Im}G_{\alpha\beta}(\vec{r}_0,\vec{r}_0;\omega)\mathrm{Im}\alpha_{\alpha\beta}^0(\omega')}{\omega+\omega'}\,. \tag{2.12}$$

Two final simplifications are possible, which are due to the fact that $G_{\alpha\beta}$ and $\alpha_{\alpha\beta}$ can be identified as susceptibilities for the field and atom, respectively, using linear-response theory.[4,5] First applying the Kramers-Kronig relations[14] for a generalized susceptibility to $G_{\alpha\beta}$, Eq. (2.12) reduces to

$$\delta E_0=-\frac{\hbar}{2\pi}\mathrm{Im}\int_0^\infty d\omega\,G_{\alpha\beta}(\vec{r}_0,\vec{r}_0;\omega)\alpha_{\alpha\beta}^0(\omega)\,. \tag{2.13}$$

Second, we apply the following transformation. We assume that $\lim_{t\to\infty}G_{\alpha\beta}(t)\to0$, which, in frequency space can be guaranteed by the addition of a small negative imaginary part to ω. This serves to lower any poles that sit on the real axis as well as to bind the integrand of (2.13) as $|\omega|\to\infty$. Since $G_{\alpha\beta}(\vec{r}_0,\vec{r}_0;\omega)$ and $\alpha_{\alpha\beta}(\omega)$ are analytic in the upper-half plane, we may convert the integral along the positive real ω axis in (2.13) to one along the positive imaginary axis, giving

$$\delta E_0=-\frac{\hbar}{2\pi}\int_0^\infty d\xi\,G_{\alpha\beta}(\vec{r}_0,\vec{r}_0;i\xi)\alpha_{\alpha\beta}^0(i\xi)\,, \tag{2.14}$$

where we have used the fact that susceptibilities evaluated at imaginary frequencies are purely real.[5] Finally, note that we are only interested in the part of the energy shift due to the presence of the surface (and/or other atoms, etc.). Setting

$$G_{\alpha\beta}=G^0_{\alpha\beta}+G^R_{\alpha\beta}\ , \tag{2.15}$$

where $G^0_{\alpha\beta}$ is the vacuum susceptibility, we can identify the energy shift of interest as

$$\delta E_0=-\frac{\hbar}{2\pi}\int_0^\infty d\xi\, G^R_{\alpha\beta}(\vec{r}_0,\vec{r}_0;i\xi)\alpha^0_{\alpha\beta}(i\xi)\ . \tag{2.16}$$

Returning now to the transition rate given by Eq. (2.5), it is useful to normalize R_{fi} to the value it would take if the atom were in vacuum at $T=0$,

$$R^0_{fi}=\frac{2}{\hbar}\mu^{fi}_\alpha\mu^{if}_\beta \mathrm{Im}G^0_{\alpha\beta}(\vec{r}_0,\vec{r}_0;\omega_0)\ . \tag{2.17}$$

At $T=0$ K, Eqs. (2.5), (2.14), and (2.16) then combine to give

$$\frac{R_{fi}}{R^0_{fi}}=1+\frac{2}{\hbar R^0_{fi}}\mu^{if}_\alpha\mu^{fi}_\beta \mathrm{Im}G^R_{\alpha\beta}(\vec{r}_0,\vec{r}_0;\omega_0)\ . \tag{2.18}$$

Equations (2.16) and (2.18) form the basis of our calculations in the following sections.

III. SUSCEPTIBILITIES ABOVE AN ARBITRARY INTERFACE

To proceed we must evaluate the field susceptibility $G_{\alpha\beta}$ near an interface. Mehl and Schaich,[2] in their study of level shifts near a metal interface, made this calculation using complex surface impedances. Instead, we keep the problem in terms of the Fresnel coefficients for the interface. This approach is more direct, since these coefficients are the ratios of only incident and reflected *electric* fields. It also generalizes more readily to complex geometries. The atomic polarizabilities $\alpha^a_{\alpha\beta}(\omega)$ do not present insurmountable problems, there being many analytic theories for their calculation.[13]

From linear-response theory,[12,14] $G_{\alpha\beta}(\vec{r},\vec{r}';\omega)$ can be identified with the expectation value of the displacement field at $\vec{r}$ generated by a classical dipole, oscillating at frequency ω, located at $\vec{r}'$. Consider such a dipole above an interface [Fig. 1(a)]. The *electric* field at position $\vec{r}$ (above the interface) consists of direct and reflected contributions, with the direct contribution given by[15]

$$\vec{E}^0(\vec{r},\omega)=\overleftrightarrow{F}^0(\vec{r},\vec{r}_0;\omega)\cdot\vec{\mu} \tag{3.1}$$

where $\vec{\mu}$ is the amplitude of the oscillating dipole, and

$$\overleftrightarrow{F}^0(\vec{R},\omega)=[(3\hat{R}\hat{R}-\overleftrightarrow{1})(R^{-3}-i\tilde{\omega}R^{-2})+(\overleftrightarrow{1}-\hat{R}\hat{R})\tilde{\omega}^2R^{-1} -\frac{4\pi}{3}\delta(\vec{R})\overleftrightarrow{1}]\exp(i\tilde{\omega}R) \tag{3.2}$$

with $\vec{R}=\vec{r}-\vec{r}_0$ and $\tilde{\omega}=\omega/c$. We use the recent work of Sipe[16] to write the reflected field as

$$\vec{E}^R(\vec{r},\omega)=\overleftrightarrow{F}^R(\vec{r},\vec{r}_0;\omega)\cdot\vec{\mu} \tag{3.3}$$

where

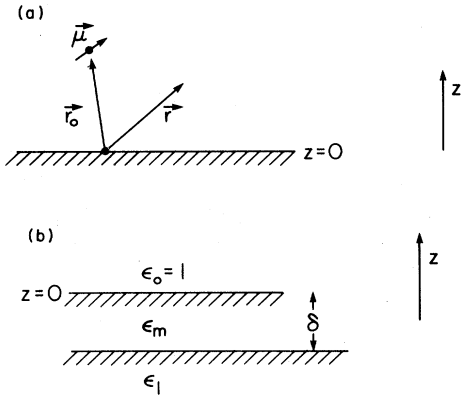

FIG. 1. Interface geometries: (a) arbitrary interface; (b) waveguide structure, with $\epsilon_m>\epsilon_1>\epsilon_0$.

$$\overleftrightarrow{F}^R(\vec{r},\vec{r}_0;\omega)=\frac{i\tilde{\omega}^2}{2\pi}\int\frac{d\vec{\kappa}}{W_0}(\hat{s}\hat{s}R^s+\hat{p}_{0+}\hat{p}_{0-}R^p) \times\exp[i(2W_0d+\vec{v}_{0+}\cdot\vec{R})] \tag{3.4}$$

with

$$\begin{aligned}&\vec{r}_0=\vec{\rho}_0+d_0\hat{z}\ ,\\ &\hat{s}=\hat{\kappa}\times\hat{z}\ ,\\ &\hat{p}_{0\pm}=\tilde{\omega}^{-1}(\kappa\hat{z}\mp W_0\hat{\kappa})\ ,\\ &\vec{v}_{0+}=\vec{\kappa}+W_0\hat{z}\ ,\\ &W_0=(\tilde{\omega}^2-\kappa^2)^{1/2}\ .\end{aligned} \tag{3.5}$$

Here R^s and R^p are, respectively, the Fresnel reflection coefficients for the interface for s- and p-polarized light. The decomposition (3.4) expresses the field as a superposition of plane waves with real wave-vector components in the plane of the interface; they are propagating or evanescent in the z direction as $\kappa<\tilde{\omega}$ or $\kappa>\tilde{\omega}$. The vectors $\hat{s}$ and $\hat{p}_{0\pm}$ specify, respectively, the direction of the electric vector in s- and p-polarized waves. In the case of p-polarization the vectors are different for upward (+) or downward (−) propagating or evanescent waves; the product $\hat{p}_{0+}\hat{p}_{0-}$ thus appears in (3.4) because the downward propagating wave is reflected back upward, with a final upward wave vector $\vec{v}_{0+}$. The phase factor $\exp(2iW_0d_0)$ also appears because of this reflection from the surface.

Since the displacement field is given, in the dipole approximation, by

$$\vec{D}(\vec{r},t)=\vec{E}(\vec{r},t)+4\pi\vec{\mu}(t)\delta(\vec{R}) \tag{3.6}$$

above the interface, we have

$$\begin{aligned}&G^0_{\alpha\beta}(\vec{r},\vec{r}_0;\omega)=F^0_{\alpha\beta}(\vec{r},\vec{r}_0;\omega)+4\pi\delta_{\alpha\beta}\delta(\vec{R})\ ,\\ &G^R_{\alpha\beta}(\vec{r},\vec{r}_0;\omega)=F^R_{\alpha\beta}(\vec{r},\vec{r}_0;\omega)\ .\end{aligned} \tag{3.7}$$

Using the first of Eqs. (3.7) in (2.16), we find the usual result[17]

$$R_{fi}^{0}=\frac{4\tilde{\omega}^{3}|\vec{\mu}^{fi}|^{2}}{3\hbar} \tag{3.8}$$

for the decay rate of an atom in free space. In the rest of our work we shall only need $G^{R}_{\alpha\beta}$, for which we require expressions for the appropriate Fresnel coefficients. As simple examples, we will assume below that macroscopic electromagnetic theory can be used to yield good approximations for those coefficients, but this is not necessary: Fresnel coefficients have been derived which incorporate microscopic surface structure.[18,19]

Consider first an interface between vacuum ($\epsilon_0=1$) and a material with dielectric constant $\epsilon_1(\omega)$. Then R^s and R^p are given simply by

$$R^{s,p}=r_{01}^{s,p}\ , \tag{3.9}$$

where

$$r_{ij}^{s}=\frac{W_i-W_j}{W_i+W_j}\ ,$$
$$r_{ij}^{p}=\frac{\epsilon_j W_i-\epsilon_i W_j}{\epsilon_j W_i+\epsilon_i W_j} \tag{3.10}$$

are the surface reflection Fresnel coefficients for s- and p-polarized light, respectively, and

$$W_i=(\epsilon_i\tilde{\omega}^{2}-\kappa^{2})^{1/2} \tag{3.11}$$

generalizing the last of Eqs. (3.5). Here, as well as there, the square root is to be chosen such that $\mathrm{Im}\,W_i\geq 0$, $\mathrm{Re}\,W_i\geq 0$ if $\mathrm{Im}\,W=0$.

For a perfect conductor, $r_{01}^{s}=-1$ and $r_{01}^{p}=+1$, and the integral in Eq. (3.4) may be done immediately. We find

$$\begin{aligned}G^{R}_{xx}(\vec{r}_0,\vec{r}_0;i\xi)&=G^{R}_{yy}(\vec{r}_0,\vec{r}_0;i\xi)\\&=(1+\sigma+\sigma^{2})e^{-\sigma}/(8d_0)^{3}\ ,\\G^{R}_{zz}(\vec{r}_0,\vec{r}_0;i\xi)&=(1+\sigma)e^{-\sigma}/(4d_0)^{3}\ ,\\G^{R}_{\alpha\beta}(r_0,r_0;i\xi)&=0,\quad \alpha\neq\beta\end{aligned} \tag{3.12}$$

where $\sigma=2\xi d_0/c$. Note that each of the physical limits $c\to\infty$, $\xi\to 0$, and $d_0\to 0$ correspond to the dimensionless variable $\sigma\to 0$.

For a more realistic model of a surface, we simply need use the appropriate expression for $\epsilon(\omega)$ in Eqs. (3.10) and (3.11). For example, in the following section we shall use the Drude model for a metal,

$$\epsilon(\omega)=1-\frac{\omega_p^{2}}{\omega(\omega+i/\tau)}\ , \tag{3.13}$$

where ω_p is the plasma frequency and τ a phenomenological collision time. The integration in (3.4) is still straightforward in principle, but must be done numerically.

In the more complicated situation of a multilayer geometry, the Fresnel coefficients may still be easily written down, in terms of the single surface coefficients (3.10). For example, in the waveguide geometry of Fig. 1(b), we have[20]

$$R_{01}^{s,p}=\frac{r_{0m}^{s,p}+r_{m1}^{s,p}\exp(2iW_m\delta)}{1-r_{m0}^{s,p}r_{m1}^{s,p}\exp(2iW_m\delta)}\ , \tag{3.14}$$

where δ is the thickness of the waveguide and ϵ_m its dielectric constant; ϵ_1 is now the dielectric constant of the substrate. Generalizations to even more complicated structures follow similarly.

IV. ENERGY SHIFTS AND TRANSITION RATES: PERFECT CONDUCTOR

As a simple example of our formalism, we first recover the well-known results for a single atom above a perfect conductor. Using

$$\alpha_{\alpha\beta}(i\xi)=\frac{2}{\hbar}\sum_{n}\frac{\omega_{n0}\mu_{\alpha}^{0n}\mu_{\beta}^{n0}}{\omega_{n0}^{2}+\xi^{2}} \tag{4.1}$$

for the polarizability of the ground state,[6] where $\omega_{n0}=\omega_n-\omega_0$, from Eqs. (2.16) and (3.12), we immediately find

$$\begin{aligned}\delta E_0=&\frac{1}{8\pi d_0^{3}}\sum_{n}|\vec{\mu}_{\parallel}^{n0}|^{2}\left[-\eta+\left[\eta\,\mathrm{Si}(\eta)-\frac{\pi}{2}\eta\right]\left[\sin(\eta)-\frac{(1-\eta^{2})}{\eta}\cos(\eta)\right]\right.\\&\left.+\eta\left[\cos(\eta)-\frac{(1-\eta^{2})}{\eta}\sin(\eta)\right]\mathrm{Ci}(\eta)\right]\\&+\frac{1}{4\pi d_0^{3}}\sum_{n}|\vec{\mu}_{\perp}^{n0}|^{2}\left[\left[\eta\,\mathrm{Si}(\eta)-\frac{\pi}{2}\eta\right]\left[\sin(\eta)+\frac{1}{\eta}\cos(\eta)\right]\right.\\&\left.+\eta\left[\cos(\eta)-\frac{1}{\eta}\sin(\eta)\right]\mathrm{Ci}(\eta)\right]\end{aligned} \tag{4.2}$$

for the correction to the Lamb shift of the ground state due to the presence of the conductor. Here $\eta=2\omega_{n0}d_0/c$, $\vec{\mu}_{\parallel}^{n0}$ and $\vec{\mu}_{\perp}^{n0}$ refer, respectively, to the components of the matrix elements parallel and perpendicular to the surface, and $\mathrm{Si}(x)$ and $\mathrm{Ci}(x)$ are the standard sine and cosine integral functions

$$\mathrm{Si}(x)=\int_0^x \frac{\sin y}{y}dy\ ,$$
$$\mathrm{Ci}(x)=-\int_x^\infty \frac{\cos y}{y}dy\ . \tag{4.3}$$

The result (4.2) agrees with Barton.[4]

From (4.2) we can easily recover the London electrostatic limit by letting $\eta\to 0$; this gives

$$\delta E_0=-\frac{1}{16d_0^3}\sum_n(|\vec{\mu}_{\parallel}^{n0}|^2+2|\vec{\mu}_{\perp}^{n0}|^2)\ . \tag{4.4}$$

The short-range limit here varies not as d_0^{-6}, as in the van der Waals energy shift of two nearby atoms,[21] but as d^{-3}: whereas in the two-atom problem the dipole induced in the second atom due to the fluctuating dipole in the first is proportional to $d_0^{-3}\vec{\mu}$, here the induced-image dipole moment in the metal is given by $\pm\vec{\mu}$; the back interaction of the induced image or polarized atom introduces an additional factor of d_0^{-3}.

The long-range limit of (4.2) can be found by an asymptotic expansion following Barton,[4] or, more simply, using a method of McLachlan's based on the form of (2.16). The exponential decay in $G^R_{\alpha\beta}(\vec{r}_0,\vec{r}_0;i\xi)$ [Eq. (3.12)] allows us to set $\xi=0$ in the polarizability appearing in Eq. (2.16), as $d_0\to\infty$; an immediate integration then gives

$$\delta E_0=-\frac{\hbar c}{8\pi d_0^4}\alpha^0_{\beta\beta}(0)\ , \tag{4.5}$$

the Casimir-Polder expression for this geometry.[22]

The transition rate is also easily obtained. Using the imaginary part of $G^R_{\alpha\beta}(\vec{r}_0,\vec{r}_0;\omega_{n0})$ [Eq. (3.12) at real frequency] we find a transition rate from an excited state to the ground state given by one of

$$\frac{R^{\perp}}{R^0}=1+3\left[\frac{\sin(\eta)}{\eta^3}-\frac{\cos(\eta)}{\eta^2}\right],$$
$$\frac{R^{\parallel}}{R^0}=1-\frac{3}{2}\left[\frac{\cos(\eta)}{\eta^2}+\left[\frac{1}{\eta}-\frac{1}{\eta^3}\right]\sin(\eta)\right], \tag{4.6}$$

depending on whether the matrix element $\vec{\mu}^{n0}$ is perpendicular or parallel to the surface. The short-range ($\eta\to 0$) result gives $R^{\perp}=2R^0$ and $R^{\parallel}=0$, as expected from image theory. The image of a dipole perpendicular to the surface points in the same direction as the dipole, leading to a radiation reaction field at the dipole equal to twice its usual value, and thus to emission at twice the usual rate. The image of a dipole parallel to the surface points in the direction opposite to the dipole, leading to a reaction field which cancels that of the dipole, preventing any radiation. The result (4.6) agrees with Power and Thirunamachandran[1] and Agarwal;[8] it, as well as the more general expressions for decay rates in the following sections, may also be derived from a purely classical calculation.[23]

V. ENERGY SHIFTS AND TRANSITION RATES: METAL SURFACE

We now turn to the more realistic problem of an atom above a metal surface. Here, for simplicity, we study the energy shift of an oscillator atom,[21] where the polarizability in the ground state is given by

$$\alpha_0(\omega)=\frac{(\hbar c)^2\alpha c}{(mc^2)(\hbar\omega_0)}\frac{\omega_0}{\omega_0^2-\omega^2}\ , \tag{5.1}$$

where ω_0 is the $1s$-$2p$ transition frequency, mc^2 is the rest energy of an electron, and α the fine-structure constant. Since the leading term in the shift, as $d_0\to 0$, varies as d_0^{-3}, we consider the dimensionless shift $\eta^3\delta E_0/\hbar\omega_0$ as a function of η, here defined as $\eta=2\omega_0 d_0/c$. Combining (2.16) and (5.1) we find

$$\frac{\eta^3\delta E_0}{\hbar\omega_0}=\frac{-4\hbar\omega_0^2\alpha}{\pi mc^2}\times\int_0^\infty d\xi\frac{[2G^R_{xx}(\vec{r}_0,\vec{r}_0;i\xi)+G^R_{zz}(\vec{r}_0,\vec{r}_0;i\xi)]d_0^3}{\xi^2+\omega_0^2}\ , \tag{5.2}$$

where $G^R_{\alpha\beta}(\vec{r}_0,\vec{r}_0;i\xi)$ is obtained by combining (3.7), (3.9)–(3.11), and (3.13). The short-range limit, $\eta\ll 1$, is given by

$$\delta E_0=\frac{-\hbar}{12\pi d_0^3}\int_0^\infty d\xi\frac{\epsilon(i\xi)-1}{\epsilon(i\xi)+1}\alpha^0_{\beta\beta}(i\xi)\ , \tag{5.3}$$

while for the long-range limit, $\eta\gg 1$, we take the polarization and dielectric constant at zero frequency (cf. Sec. IV), giving

$$\delta E_0=\frac{-\hbar c\alpha^0_{\beta\beta}(0)}{8\pi d_0^4}\ . \tag{5.4}$$

The limiting results (5.3) and (5.4) agree with those of McLachlan[5] and Mehl and Schaich.[2] From Eq. (5.3) we see that the level shift for an atom near a metal is less in magnitude than that for an atom above a perfect conductor (where $\epsilon\to\infty$). In Fig. 2(a) we compare the shift for an oscillator atom above a perfect conductor with that for the atom above a sodium surface [taking $\hbar\omega_p=5.89$ eV, $\hbar/\tau=0.13$ eV (Ref. 19)]; the long- and short-range regimes are apparent.

To now consider the decay rates from an excited state of an atom above a metal surface, we write Eqs. (2.18) and (3.8) in the form

$$\frac{R^{\perp}}{R^0}=1+\frac{12d_0^3}{\eta^3}\mathrm{Im}G^R_{zz}(\vec{r}_0,\vec{r}_0;\omega_0)\ ,$$
$$\frac{R^{\parallel}}{R^0}=1+\frac{12d_0^3}{\eta^3}\mathrm{Im}G^R_{xx}(\vec{r}_0,\vec{r}_0;\omega_0)\ , \tag{5.5}$$

where $\hbar\omega_0$ is the (unperturbed) energy difference between

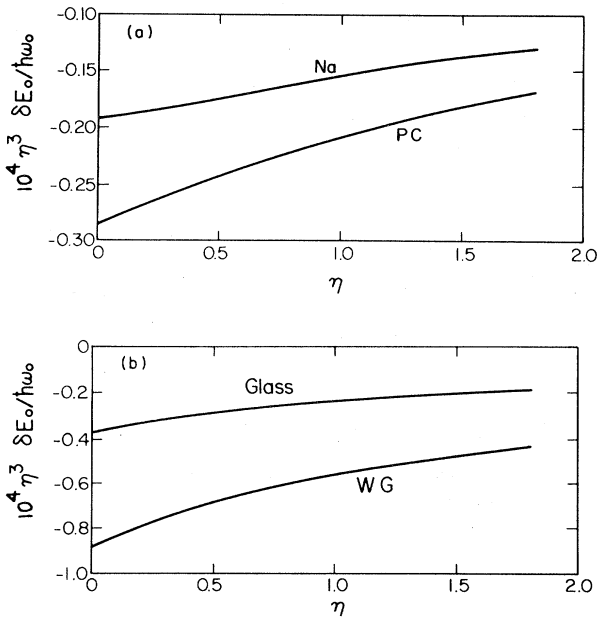

FIG. 2. Energy-level shifts: (a) correction to the level shift of the ground state of an oscillator atom, with a $2p$-$1s$ transition energy $\hbar\omega_0=2$ eV, due to the presence of a surface. For Na we let $\hbar\omega_p=5.89$ eV and $\hbar/\tau=0.13$ eV. For a perfect conductor we let $\hbar\omega_p=10^{10}$ eV and $\hbar/\tau=0$. Here $\eta=2\omega_0 d/c$ where d is the distance between the atom and the surface. (b) Same as in (a) but for a 10.2 eV transition above a glass ($\epsilon=1.69$) surface and a ZnO/sapphire waveguide ($\epsilon_m=4.08$, $\epsilon_1=3.13$, $\epsilon_0=1.00$).

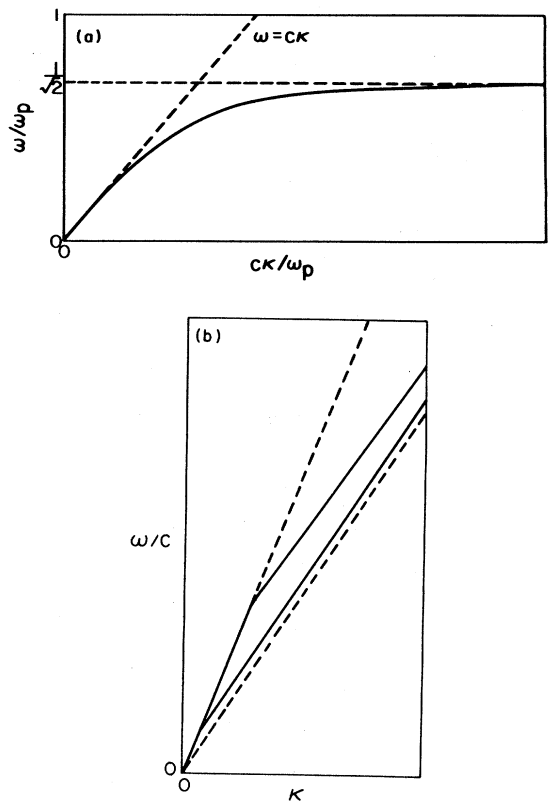

FIG. 3. Dispersion relations: (a) surface-plasmon dispersion relation in the collisionless Drude model; ω_p is the bulk plasmon frequency. (b) Waveguide dispersion relation. The upper asymptote is the bulk light line $\omega=c\kappa/\sqrt{\epsilon_1}$; the lower is the waveguide light line $\omega=c\kappa/\sqrt{\epsilon_m}$.

the initial and final states. In evaluating (5.5) numerically, care must be taken in dealing with the pole that appears in the Fresnel coefficient r_{01}^p [Eq. (3.10)] for a metal surface.[20] The pole appears at

$$\kappa=\tilde{\omega}\left[\frac{\epsilon}{\epsilon+1}\right]^{1/2} \tag{5.6}$$

and signals the presence of the surface-plasmon excitation; the well-known dispersion relation for surface plasmons in the $\tau\to\infty$ limit is shown in Fig. 3(a). A simple method is to remove the pole in the integrand of Eq. (3.4) and evaluate its contribution analytically; the rest of the integrand is a slowly varying function of κ and its numerical integration is straightforward.

In Figs. 4(a) and 4(b) we compare the decay rates for an atom above a perfect conductor with those for an atom above a sodium surface. In the latter case we have fixed the transition frequency at $\omega_0/\omega_p=0.7$, which is just below $\omega_0/\omega_p=1/\sqrt{2}$ [see Fig. 3(a)], and guarantees near resonance with large-κ surface plasmons. However, regardless of the value of ω_0 chosen, the rates over a metal show a divergence as $\eta\to 0$ which is not present for the perfect conductor. We can understand this classically by noting that the dissipation in the metal—manifested by an imaginary part in the dielectric constant—will cause the image dipole to have a component out of phase with the real dipole, and therefore out of phase with the near field of the dipole. The near field, therefore, does work on the image dipole in this simple picture, which physically describes the dissipation occurring near the surface, and provides a decay mechanism for the atom. Since the near field diverges as $r\to 0$, so does the rate at which the energy can leave the atom. We note that this divergence is not directly connected with the surface-plasmon excitations; it would exist for any surface with dissipation and therefore a complex dielectric constant, even if the material were an essentially dispersionless dielectric. The shoulder in Fig. 4(b) at $\eta\sim 3$ arises as the finite, image theory result for a perfect conductor is surpassed by this divergence. If the dissipation is removed ($\tau\to\infty$), the shoulder becomes more pronounced and [except for $\omega_0/\omega_p=1/\sqrt{2}$] the rates remain finite at all η.

However, there is a divergent effect due specifically to the surface plasmons. Even in the absence of dissipation, if $\eta\to 0$ the rates diverge for the special transition frequency $\omega_0/\omega_p=1/\sqrt{2}$. This occurs because of the infinite density of states of surface plasmons in this model at that frequency [see Fig. 3(a)]. As $\eta\to 0$, the evanescent part of the field [Eq. (3.3)] from the dipole at values of $\kappa>\tilde{\omega}$ can couple the atom into more and more of these decay channels. This divergence was noted years ago by Morawitz and Philpott.[23] We emphasize here that it occurs only if $\omega_0/\omega_p=1/\sqrt{2}$ although, of course, if ω_0/ω_p is near $1/\sqrt{2}$ the coupling with surface plasmons will lead to an increase in the decay rates over their values

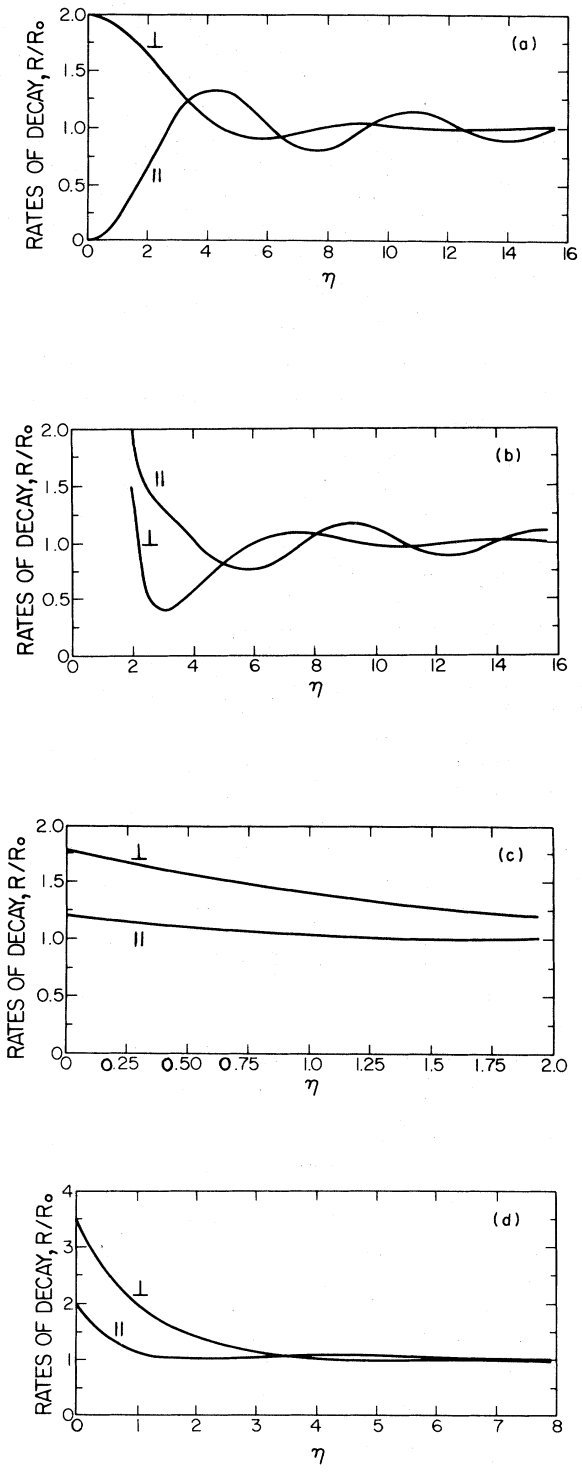

FIG. 4. Rates of decay: (a) dipole transition rates, normalized to the free-space rate R_0, for dipoles oriented parallel and perpendicular to the plane of a perfectly conducting surface. (b) Same as for (a) but a 4.123 eV transition above a Na surface. The transition frequency was chosen so that $\omega_0 \leq \omega_p/\sqrt{2}$. (c) Same as for (a) but for an arbitrary dipole transition above a glass surface. (d) Same as for (a) but for an arbitrary dipole transition above a ZnO/sapphire waveguide. The waveguide thickness δ [Fig. 1(b)] was chosen so that only one s and one p mode could exist for a transition energy of $\hbar\omega_0$.

for a perfect conductor. In the absence of dissipation, as $\omega_0/\omega_p \to 1/\sqrt{2}$, the rates at $\eta=0$ diverge as $[\epsilon(\omega_0)+1]^{-5/2}$.

Thus, we can identify two physical contributions to the decay rate divergences as $\eta \to 0$. The first is due to dissipation; the second is due to coupling into surface plasmons and occurs as $\omega_0/\omega_p \to 1/\sqrt{2}$. From Eq. (3.13) we see that if the transition frequency ω_0 is well above $\omega_p/\sqrt{2}$ and there is finite dissipation, the rates behave essentially like free-space rates, but with a dissipation divergence for $\eta \ll 1$. For transition frequencies ω_0 well below $\omega_p/\sqrt{2}$, the rates behave very much like those for a perfect conductor but again, with a dissipation divergence for $\eta \ll 1$.

Of course, both the dissipation and surface-plasmon divergences discussed here will in reality be ameliorated by microscopic effects: First, as $\eta \to 0$ the charge distribution of the atom will begin to overlap with that of the surface, and our model of a point dipole above a sharp interface will break down.[24] Second, more microscopic calculations of the surface-plasmon dispersion relation indicate a finite density of states at all frequencies, as ω deviates from $\omega_p/\sqrt{2}$ and as κ increases.[25] Nonetheless, the calculations presented in Fig. 4(b), and similar ones for other values of the important parameters, indicate that there are distances above the surface where the presence of the surface will modify the energy shifts and transition rates, and yet where our simple model should constitute at least a good first approximation.

VI. ENERGY SHIFTS AND TRANSITION RATES: WAVEGUIDE INTERFACE

Now let us turn to a different but related problem: an atom over a dielectric waveguide [Fig. 1(b)] with dielectric constants taken to be real, greater than one, and frequency independent. We use Eqs. (3.4), (3.7), (3.14), and (5.2) to calculate the correction to the ground-state energy-level shift of an oscillator atom due to the presence of a ZnO/sapphire waveguide. In Fig. 2(b) we compare this shift to that for an atom above a glass ($\epsilon=1.69$) surface; once again we see the long- and short-range regimes explicitly, as in the metal calculation. Qualitatively, there is not much difference between the single surface and the waveguide.

For the decay rates we use Eqs. (3.4), (3.7), (3.14), and (5.5). In the integrands of (3.4) there are poles, here in general in both of R^p_{01} and R^s_{01}; these signal the presence of the waveguide modes, and the number of "s" and "p" modes depends on the thickness of the guide. To conveniently evaluate the expressions (5.5) we proceed as in the surface-plasmon example: the pole contributions are evaluated analytically, leaving a slowly varying function of κ which can easily be evaluated numerically. In the analytic evaluation we add a positive infinitesimal imaginary part to the waveguide mode wavenumbers, which ensures the boundary condition at $|\vec{R}| \to \infty$ of waveguide modes carrying energy away from the atom.

In Figs. 4(c) and 4(d) we show, respectively, the decay rates for an atom above a glass surface, and above a ZnO/sapphire waveguide, with a thickness chosen to al-

low one s and one p mode to exist. In neither case is there a "dissipation divergence," since we have taken all dielectric constants to be real. For glass, the rates remain small, as there are no surface excitations. The presence of waveguide modes as surface excitation decay channels enhances the decay rates for the waveguide geometry, as did surface plasmons in the metal-surface example. The magnitude of the rates are smaller here than in the sodium calculation, partly because of our choice of the waveguide material: the pole strengths for the waveguide modes are proportional to $(\epsilon_m - 1)^{-1}$, and ZnO gives a fairly large $\epsilon_m = 4.08$. Further, though, it is important to note that there is nothing analogous to the "surface-plasmon divergence" in the example of a waveguide: the dispersion relation for the waveguide modes [Fig. 3(b)] does not yield an infinite density of states of surface excitations at any frequency. Thus, although surface plasmons and waveguide modes can affect certain attenuated-total-reflection experiments in a similar way,[26] since they can lead to similar pole strengths in the respective Fresnel coefficients, they affect the decay of excited states of atoms above the surface in quite different manners.

Additional calculations show that, although increasing the thickness of the guide allows more decay channels to exist in the form of more waveguide modes, there is little effect on the transition rates. This occurs partly because the wave number of a given mode increases as the waveguide thickness is increased; the component of the field which couples into that mode is thus more evanescent and, for a given atom-surface distance and a given mode, the coupling will be less as the waveguide thickness increases. Further, the pole strength of a given mode decreases as the waveguide thickness gets well beyond the cut-off thickness for that mode, decreasing the intrinsic strength of the coupling.[26] Finally, from Eq. (3.14), we see that for large κ, the magnitude of the image dipole in the waveguide decreases with an increase in the waveguide thickness.

VII. CONCLUSION

We have presented a general formalism for calculating level shifts and decay rates for atoms and molecules in the presence of, but not with charge distributions that overlap with, an arbitrary interface. The essential point is to construct expressions for the level shifts and decay rates in terms of the appropriate response functions of the interface, which here involve the Fresnel coefficients. This separates the intrinsic physics of the decay rate and level shift from the physics of the particular interface under consideration. The first of these is embodied in our general expressions; the second, insofar as it is important for our results, resides in the Fresnel coefficients, the poles of which signal and describe the contributions of any surface excitations of relevance. For any new surface or general interface of interest, only the new Fresnel coefficients need now be supplied. The decay rates and level shifts immediately follow; the general calculation need not be undertaken again.

As specific examples, we have considered atoms above a metal surface, using the simple, but not totally unrealistic Drude model, and atoms above a glass surface and a waveguide in the dissipation-free limit. We have shown that, because of their qualitatively different dispersion relations, surface plasmons and waveguide modes have qualitatively different effects on the decay rates of nearby atoms.

In this paper we have treated only the problem of one atom or molecule above an interface, but McLachlan[6] has shown that the linear-response formalism (Sec. II) can be simply extended to treat two or more bodies. Combining this with the field decomposition of Sec. III, it is easy to recover the Lamb shift of two atoms above a perfect conductor, as calculated in a more direct but algebraically more complicated approach by Power and Thirunamachandran.[1] The details of such matters we here defer, as we plan to discuss the physics of many atoms above arbitrary interfaces in future publications. We here merely note that recent experimental[3] and theoretical[1,2] interest in problems of this sort suggests that general formalisms of the type we have developed here will be of some use. In particular, the extension of this formalism to treat level shifts of *excited states* is an outstanding problem[27] which we plan to address.

ACKNOWLEDGMENTS

This work is supported by the Natural Sciences and Engineering Research Council of Canada, including a postgraduate scholarship to one of us (J.M.W).

[1] E. Power and T. Thiunamachandran, Phys. Rev. A **25**, 2473 (1982).
[2] M. J. Mehl and W. L. Schaich, Surf. Sci. **99**, 553 (1980).
[3] P. Goy, J. M. Raimond, M. Gross, and S. Haroche, Phys. Rev. Lett. **50**, 1903 (1983).
[4] G. Barton, J. Phys. B **7**, 2134 (1974).
[5] A. D. McLachlan, Proc. R. Soc. London, Ser. A **271**, 387 (1963).
[6] A. D. McLachlan, Mol. Phys. **6**, 423 (1963); *ibid.* **7**, 381 (1963).
[7] G. S. Agarwal, Phys. Rev. A **11**, 230 (1975).
[8] G. S. Agarwal, Phys. Rev. A **12**, 1475 (1975).
[9] E. Power and S. Zienau, Philos. Trans. R. Soc. London A **251**, 427 (1959).
[10] W. P. Healy, Phys. Rev. A **22**, 2891 (1980).
[11] H. Bethe, Phys. Rev. **72**, 339 (1947).
[12] E. M. Lifshitz and L. P. Pitaevskii, *Statistical Physics,* 3rd ed., (Pergamon, New York, 1980), Part One, pp. 377–396.
[13] G. Lamm and A. Szabo, J. Chem. Phys. **72**, 3354 (1980).
[14] R. B. Stinchcombe, *Correlation Functions and Quasiparticle Interactions in Condensed Matter,* edited by J. Hailey (Plenum, New York, 1978), pp. 3–45.
[15] J. D. Jackson, *Classical Electrodynamics,* 2nd ed. (Wiley, New York, 1975), pp. 141, 395, 311, and 344.
[16] J. E. Sipe, Surf. Sci. **105**, 489 (1981).
[17] P. A. M. Dirac, *The Principles of Quantum Mechanics,* 4th ed. (Oxford, London, 1967), p. 245.

[18]J. E. Sipe, Phys. Rev. B **22**, 1589 (1980).
[19]J. E. Sipe, Surf. Sci. **84**, 75 (1979).
[20]J. E. Sipe, J. Opt. Soc. Am. **72**, 2 (1982).
[21]L. I. Schiff, *Quantum Mechanics* (McGraw-Hill, New York, 1968), p. 261.
[22]H. R. G. Casimir and D. Polder, Phys. Rev. **73**, 360 (1948).
[23]H. Morawitz and M. R. Philpott, Phys. Rev. B **10**, 4863 (1974).
[24]B. N. J. Persson, J. Phys. C **11**, 4251 (1978).
[25]J. Harris and A. Griffin, Phys. Rev. B **3**, 749 (1971).
[26]J. E. Sipe and J. Becher, J. Opt. Soc. Am. **72**, 288 (1982).
[27]M. Babiker and G. Barton, J. Phys. A **9**, 129 (1976).